Comparison of C_{60} encapsulations into carbon and boron nitride nanotubes

2004 J. Phys.: Condens. Matter 16 3901

(http://iopscience.iop.org/0953-8984/16/23/010)

INSTITUTE OF PHYSICS PUBLISHING JOURNAL OF PHYSICS: CONDENSED MATTER

J. Phys.: Condens. Matter **16** (2004) 3901–3908 PII: S0953-8984(04)75541-1

Comparison of C_{60} encapsulations into carbon and boron nitride nanotubes

Jeong Won Kang and Ho Jung Hwang

Department of Electronic Engineering, Nano Electronic and Future Technology Laboratory, Chung-Ang University, 221 HukSuk-Dong, DongJak-Ku, Seoul 156-756, Korea

E-mail: gardenriver@korea.com (J W Kang) and hjhwang@cau.ac.kr (H J Hwang)

Received 28 January 2004
Published 28 May 2004
Online at stacks.iop.org/JPhysCM/16/3901
DOI: 10.1088/0953-8984/16/23/010

Abstract

This work, by means of molecular dynamics simulations, shows that the features of C_{60} encapsulation into boron nitride nanotubes (BNNTs) are similar to the features of that into carbon nanotubes (CNTs), whereas the encapsulating and the internal dynamics of the C_{60}@BNNT are different from those of the C_{60}@CNT. Since the C_{60} encapsulation into the BNNTs is energetically more stable than that into the CNTs and the suction force on the C_{60} molecule induced by the BNNTs is higher than that by the CNTs, the C_{60} encapsulation into the BNNT is achieved faster than that into the CNT. The internal dynamics of the C_{60} molecule inside the BNNT is also different from that inside the CNT, because the C_{60}@CNT system includes only one long range interaction of C–C whereas the C_{60}@BNNT system includes both C–B and C–N long range interactions. Because of the difference of the binding energies and the equilibrium distances between C–B and C–N, the C_{60} molecule frequently collided against the BNNT wall in molecular dynamics simulations. At low temperature, the energy dissipation of the C_{60}@CNT system mainly occurred at both end edges of the CNT, where the C_{60} molecule is under restoring (or sucking-in) forces. Energy dissipation of the C_{60}@BNNT resulted from collisions against the BNNT wall as well as at both end edges of the BNNT.

(Some figures in this article are in colour only in the electronic version)

The large empty space inside carbon nanotubes (CNTs) or boron nitride nanotubes (BNNTs) has opened new application areas such as in storage materials with high capacity and stability. These cavities are large enough to accommodate a wide variety of atomic and molecular species that can significantly influence the properties of the materials. In particular, self-assembled hybrid structures called 'carbon nanopeapods (C-NPs)' have been reported [1–7]. The application of nanopeapods ranges from use as nanometre-sized containers of chemical

reactant [5] to use for date storage [8] and in high temperature superconducting [9]. Berber *et al* [10] also showed that the encapsulation process did not involve an activation energy barrier, using tight-binding MD simulations. Qian *et al* [11] showed that C_{60} was sucked into the (10, 10) CNT by the sharp surface tension force presented at the front of the open end and then oscillated between the two open ends of the CNT, never escaping. It has been proposed that encapsulation can be either through the ends of oxidatively opened single-wall CNTs or through defects in their sidewalls. The different formation mechanisms of the C-NPs have been extensively investigated and discussed by Ulbricht and Hertel [12].

Recently, 'boron nitride nanopeapods (BN-NPs)' were also synthesized [13]. *Ab initio* calculations showed that the exothermic energy of a C_{60}@(10, 10) BNNT, 1.267 eV, is higher than that of a C_{60}@(10, 10) CNT, 0.508 eV [14]. This result implies that the formation of the BN-NPs is easier than the formation of the C-NPs. The importance of the BN-NPs is not only the possibility of easy formation but also the dramatic variations of their electronic properties. The E_g of the (10, 10) BNNT is 4.5 eV whereas the E_g of its BN-NP is 1.3 eV [14]. Ulbricht and Hertel [12] have investigated various mechanisms of formation of the C-NPs using molecular dynamics and kinetic Monte Carlo trajectory calculations. They compared the capture of ballistic C_{60} from the gas phase with encapsulation of C_{60} preadsorbed on the surface of single-wall CNT ropes; and then they predicted that the encapsulation of the preadsorbed C_{60} was more likely to be achieved than encapsulation of the gas phase. They also showed that encapsulations through tube ends were more likely than encapsulations through the sidewall defects on the single-wall CNTs. However, to the best of our knowledge, the formation dynamics of the BN-NPs has not been investigated except in the work by Okada *et al* [14]. In the discussion by Grifalco and Hodak [15], the van der Waals binding energies by Okada *et al* are much too low, comparing with other theoretical and experiment works.

Here, we study the mechanism of nanopeapod formation using molecular dynamics simulations. We compare the formation mechanism and the internal dynamics of the BN-NP with those of the C-NP.

For carbon–carbon interactions, we used the Tersoff–Brenner potential function [16–18] that has been widely applied in carbon systems. The long range interactions of carbon were characterized with the Lennard-Jones 12–6 (LJ12–6) potential with the parameters obtained from the experimental result for the C_{60}–graphite system by Ulbricht *et al* [19]. For boron nitride interactions, we used the Tersoff potential with parameters fitted by Albe and Moller [20]. Although the drawback of the Tersoff-type potential is that it cannot describe ionic interaction between boron and nitrogen, this potential was effectively applied to the boron nitride nanotubes [21]. The long range interactions of boron and nitrogen were also characterized with the LJ12–6 potential with the parameters from the force fields in DERIDING/A [22]. In this work, the parameters for the LJ12–6 potential are $\varepsilon_{\mathrm{Carbon}} = 0.002\,635$ eV, $\sigma_{\mathrm{Carbon}} = 3.369$ Å, $\varepsilon_{\mathrm{Boron}} = 0.004\,116$ eV, $\sigma_{\mathrm{Boron}} = 3.453$ Å, and $\varepsilon_{\mathrm{Nitrogen}} = 0.006\,281$ eV, $\sigma_{\mathrm{Nitrogen}} = 3.365$ Å, respectively. The carbon–boron and carbon–nitrogen parameters were derived using the Lorentz–Berthelot mixing rules, $\varepsilon_{\mathrm{AB}} = \sqrt{\varepsilon_{\mathrm{A}}\varepsilon_{\mathrm{B}}}$ and $\sigma_{\mathrm{AB}} = (\sigma_{\mathrm{A}} + \sigma_{\mathrm{B}})/2$. The cut-off distances for all cases are 15 Å in this work.

We used both steepest descent (SD) and MD methods. The MD simulations used the same MD methods as were used in our previous works [23–25]. The MD code used the velocity Verlet algorithm, and neighbour lists to improve computing performance [26]. MD time step was 5×10^{-4} ps. Initial velocities were assigned from the Maxwell distribution and the magnitudes were adjusted so as to keep the temperature in the system steady. A Gunsteren–Berendsen thermostat was used to control temperature for all atoms except for fullerenes [26].

Figure 1 shows the energetics of the C_{60} molecule encapsulation into a (10, 10) nanotube as a function of the central position (Z_{centre}) of the C_{60} molecule along the tube axis (z-axis).

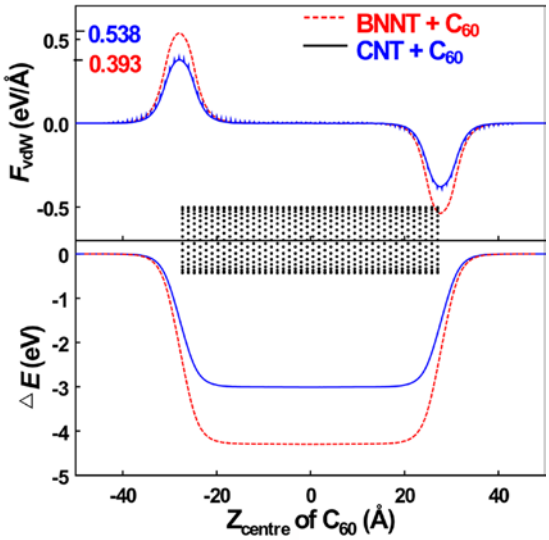

Figure 1. The van der Waals forces (F_{vdW}) and formation energetics (ΔE) of the C_{60} molecule encapsulation into a (10, 10) nanotube as a function of the central position (Z_{centre}) of the C_{60} molecules along the tube axis (z-axis).

The (10, 10) nanotube with 54 Å length was initially optimized by an annealing simulation. The centre of the nanotube along the tube axis was located at zero as shown in figure 1; and then the Z_{centre} of a C_{60} molecule was increased by 0.1 Å from −50 to 50 Å. At each position, the processes of relaxation by the SD method were performed under the condition that the central position of the nanotube was always zero and the central position of the C_{60} was fixed. The bottom figure in figure 1 shows the formation energies of the C_{60} encapsulation. The formation energy of a C_{60}@CNT is 3.02 eV. This value is similar to the value, 3.01 eV, obtained from the work by Ulbricht *et al* [19]. The value 3.26 eV obtained from the work by Girifalco *et al* [27] is slightly higher than the value in this work, because the potential well depth used in this work is slightly lower than those used by Girifalco *et al* [28]. This value is generally around 3 eV. However, the value 11.881 eV given by Qian *et al* [11] who investigated using a Morse-type potential based on a local density approximation (LDA) calculation is very much higher than other results. However, the value 0.508 eV given by Okada *et al* [14] is very smaller than other results such as those discussed by Girifalco and Hodak [15]. The formation energy of a C_{60}@BNNT is 4.383 eV in this work. This value is higher than that for C_{60}@CNT. In the results given by Okada *et al* [14], the formation energy of a C_{60}@BNNT is higher than that of a C_{60}@CNT. Although the quantities of the exothermic energy obtained from Okada *et al* [14] are still open to doubt [15], their results are similar to our results: that the formation of the BN-NP is energetically easier than the formation of the C-NP. Okada *et al* [14] discussed the feature that the hybridization between the nearly free electron (NFE) states of BNNT and the π orbitals of C_{60} can induce a large energy gain upon the encapsulation of the C_{60}s in the BNNT. Although they showed that the electrons were transferred mainly from the π orbitals of both the BNNT and the C_{60} to the space between the BNNT and the C_{60}, the charge transfer from the π orbitals of the BN-NP was similar to that of the C-NP. Therefore, the large exothermal energy of the BN-NP should be attributed to another reason. Since the B–N bonds composed of the BNNT have polar nature and the π orbitals of the BNNT are distributed on the N atomic sites, it is clear that both the cation B–C and the anion N–C long range interactions are different from

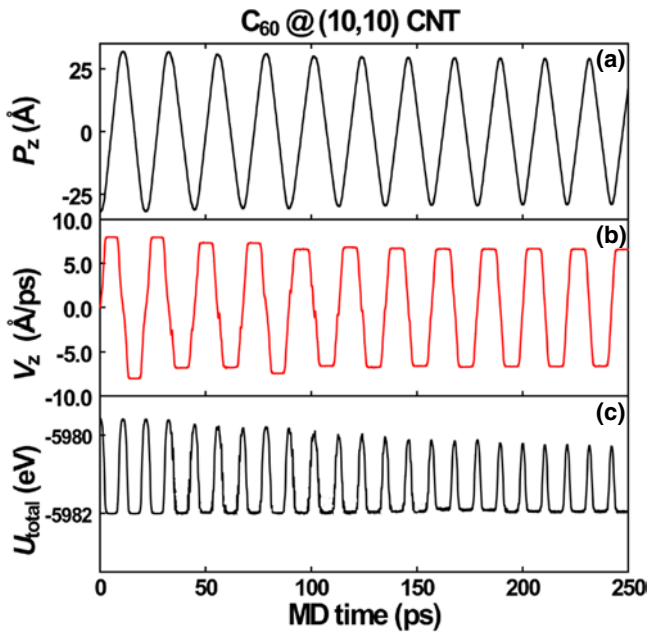

Figure 2. MD simulations for a C_{60} molecule encapsulation of a (10, 10) CNT induced by the suction forces (F_{vdW}) at the edge of the nanotube. A C_{60} molecule was initially located at -32 Å and then MD simulations were performed at 10 K for 500 ps, neglecting the thermal surface wave effect of the nanotubes. (a) The central position (P_Z) and (b) velocity (V_Z) of the C_{60} molecule along the tube axis and (c) the total potential energy (U_{total}) variations as a function of MD time.

the C–C van der Waals interactions. Detailed study for the interactions between the BNNT and the encapsulated C_{60} should be performed using *ab initio* calculations.

The upper figure in figure 1 shows the van der Waals forces (F_{vdW}) exerted on the C_{60} molecule. The F_{vdW}s directly obtained from the atomistic simulations are the same as the F_{vdW}s obtained from the deviation of the formation potential energy variation, $-d\Delta E/dz$, where ΔE is the formation energy of C_{60}+ nanotube. However, the values of $F_{vdW} = -d\Delta E/dz$ show several small peaks along the tube axis as shown in figure 1. The period of these small peaks is exactly as with the distance between carbon rings for the tube axis. Since the F_{vdW} is a suction force, a C_{60} molecule is automatically sucked into the nanotube when it comes up close to the open end of the nanotubes. The maximum F_{vdW} of the C_{60}-(10, 10) BNNT case (5.38 eV Å^{-1}) is higher than that of the C_{60}-(10, 10) CNT case (0.393 eV Å^{-1}).

Figures 2 and 3 show the results of the MD simulations for a C_{60} molecule encapsulation of a (10, 10) CNT and a (10, 10) BNNT induced by the suction forces at the edge of the nanotube, respectively. A C_{60} molecule was initially located at -32 Å and then the MD simulations were performed at 10 K for 500 ps, neglecting the thermal surface wave effect of the nanotubes. The constraint dynamics was applied to the nanotubes. The potential energies (figures 2(c) and 3(c)) in the initial configuration were transferred to the kinetic energies (figures 2(b) and 3(b)). This energetics is the same as that discussed in figure 1. The transfers between potential and kinetic energies make this system oscillate like a spring or an actuator. As shown in figure 1, since the force F_{vdW} of sucking of the C_{60} into the BNNT is higher than that into the CNT, the oscillation frequency of the C_{60}, 60 GHz, in the BNNT is also higher than that, 45 GHz, in the CNT below 150 ps as shown in figures 2 and 3. In classical oscillation theory $\Delta F = k\Delta x$; when the

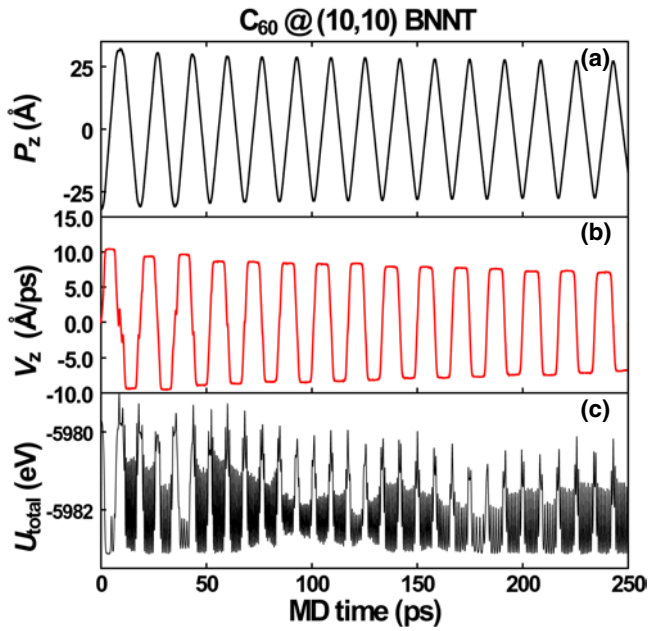

Figure 3. MD simulations for a C_{60} molecule encapsulation of a (10, 10) BNNT induced by F_{vdW} at the edge of the nanotube. A C_{60} molecule was initially located at -32 Å and then the MD simulations were performed at 10 K for 500 ps, neglecting the thermal surface wave effect of the nanotubes. The long range interactions of C–B and C–N were calculated using corresponding parameters. (a) P_Z, (b) V_Z, and (c) U_{total} variations as a function of MD time.

C_{60} oscillation is initialized at both end edges, k_{BNNT} and k_{CNT} are 0.032 and 0.023 nN Å^{-1}, respectively. From the classical theory $\Delta U = \frac{1}{2}k(\Delta x)^2$, when the C_{60} oscillation is initialized beyond 8 Å from the left end edge, k_{BNNT} and k_{CNT} are 6.795×10^{-3} and 4.757×10^{-3} nN Å^{-1}, respectively.

Since these MD simulations were performed at very low temperature, the energy dissipation, due to the collisions against the nanotube wall, was very small. However, energy dissipation at both end edges, where the C_{60} molecule is under restoring (or sucking-in) forces, can be found as several small distortions of the velocity (V_Z) variation of the C_{60} molecule along the tube axis. In our MD simulations, this energy dissipation was found when the central position (P_Z) variations of the C_{60} molecule are over both end edges. Therefore, when the maximum of the P_Z of the C_{60} molecule is below both end edges, the oscillation features are almost stable. These results are in good agreement with previous work [11] and with a recent result for a carbon oscillator [28–30]. In our MD simulations, the stable oscillations of the C_{60} inside the CNT were found after 200 ps. The internal dynamics of a C_{60} inside the BNNT is different from that of a C_{60} inside the CNT in the aspect of variations of the total potential energy of the system U_{total}. Since the C_{60} molecule inside the CNT came and went smoothly in general, the energy dissipation was mainly found when the P_Z of the C_{60} molecule were over both end edges and the plot of the U_{total} was also smooth on the whole. However, in the BNNT, since the C_{60} molecule collided against the tube wall several times while penetrating the tube, many peaks are found in the plot of U_{total}. Therefore, V_Z for the C_{60} molecule is continually decreased due to the damping effects. Thus difference is due to the structural difference as well as the different long range interactions; i.e. the BNNTs are composed of binary atoms

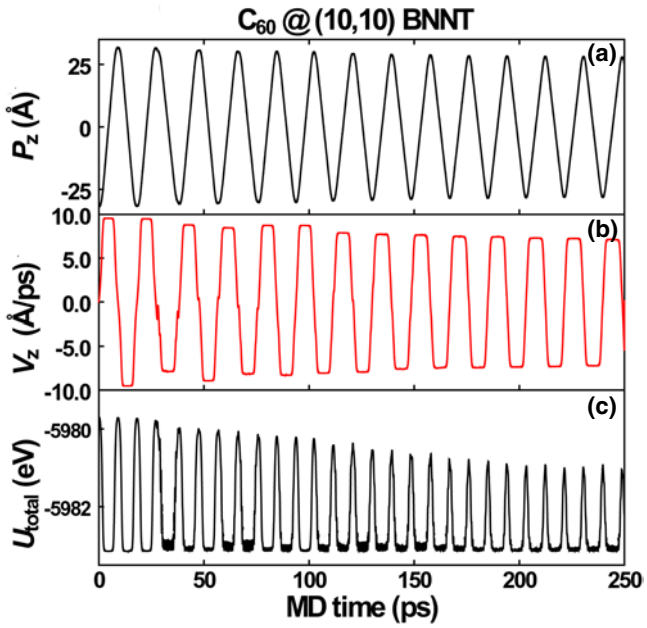

Figure 4. MD simulations for a C_{60} molecule encapsulation of a (10, 10) BNNT induced by F_{vdW} at the edge of the nanotube. A C_{60} molecule was initially located at -32 Å and then the MD simulations were performed at 10 K for 500 ps, neglecting the thermal surface wave effect of the nanotubes. The long range C–BN interactions were calculated by means of a single parameter set using the Lorentz–Berthelot mixing rules. (a) P_Z, (b) V_Z, and (c) U_{total} variations as a function of MD time.

whereas the CNTs are composed of the element atoms. In the MD simulations, symmetric optimization between a CNT and a C_{60} can be easily achieved from just one LJ12–6 potential function for the long range interactions, whereas that between a BNNT and a C_{60} is hardly achieved from two LJ12–6 potentials for different long range interactions, because the C–B and C–N equilibrium distances in the force field DERIDING/A [22] are 3.828 and 3.779 Å, respectively. To confirm our discussion, we performed MD simulations with a single C–BN parameter set. The parameters for the LJ12–6 potential were

$$\varepsilon_{C-BN} = \sqrt{\varepsilon_{C-B}\varepsilon_{C-N}} = 0.003\,66\ \text{eV} \qquad \text{and} \qquad \sigma_{C-BN} = (\sigma_{C-B} + \sigma_{C-N})/2 = 3.389\ \text{Å}. \tag{1}$$

Figure 4 shows that the dynamics of the C_{60} inside the BNNT was similar to that inside the CNT as shown in figure 2 except for the different quantities such as frequencies and magnitudes. In figure 4, though the C_{60} molecule collided against the tube wall several times during penetration of the BNNT, the effects of the collisions are similar to the case of figure 2 rather than the case of figure 3. Figure 4 also shows that the energy dissipation due to the collisions between the C_{60} molecule and the BNNT wall affected P_Z, U_{total}, and V_Z variations. The average energy dissipation rates for figures 2–4 are 0.0032, 0.0068, and 0.0064 eV ps^{-1}, respectively. Therefore, the average energy dissipation rate of the C_{60} inside the BNNT is twice higher than that of the C_{60} inside the CNT. This result can be explained by the difference in long range interactions and the difference in atomic mass. The potential well depths of the LJ12–6 function for the C–BN long range interactions are higher than those for the C–C long range interactions. Since the N atomic mass is greater than the B atomic mass, the N atoms are more

slowly accelerated than the B atoms. Therefore, the energy dissipation of the C_{60} inside the BNNT composed of binary atoms was slightly different from that inside the CNTs composed of the element atoms. For the collisions between the BNNT wall and the encapsulated C_{60}, the features of the dynamics of the MD simulations using the C–BN parameter set were different from those when using both C–B and C–N parameter sets. However, the average energy dissipations of the two cases were very similar to each other. Considering that the dynamics of the C_{60} inside the BNNT as shown in figure 4 was similar to that inside the CNT as shown in figure 2 except for the different quantities such as frequencies and magnitudes, we can conclude that the energy dissipations of the C_{60} inside the BNNT are mainly influenced by the difference in long range interaction rather than the difference in atomic mass between B and N. Our MD simulations show that to investigate the internal dynamics of C_{60} molecules inside the BNNTs, the potential functions for the long range interactions will have to be carefully adopted.

As the MD temperature increases, the energy dissipation of the C_{60} oscillation may increase because the friction effects caused by the radial breathing modes of nanotubes increase. Since the binding energy of the BNNTs is lower than that of the CNTs, the thermal vibration and the breathing of the BNNTs can affect more than those of the CNTs the internal dynamics and the energy dissipation of the encapsulated C_{60} molecules. Further works including ones on packing structures and temperature effects will form a more detailed investigation of the dynamics of encapsulation of the C_{60} molecules into the BNNT.

In summary, though the features of the C_{60} encapsulation into the BNNT are similar to those of encapsulation into the CNT, the encapsulating and the internal dynamics of the C_{60}@BNNTs are different from those of the C_{60}@CNTs. Since the suction force on the C_{60} molecule induced by the BNNTs is higher than that induced by the CNTs, the C_{60} encapsulation into the BNNT is achieved faster than that into the CNT. The C_{60} encapsulation into the BNNTs is energetically more stable than that into the CNTs. The internal dynamics of the C_{60} molecule inside the BNNT is also different from that inside the CNT, because the C_{60}@CNT system includes only one long range interaction of C–C whereas the C_{60}@BNNT system includes both C–B and C–N long range interactions. Since the C–B and C–N interaction energies and equilibrium distances are different from each other, the C_{60} molecule frequently collides against the BNNT wall in our MD simulations. At low temperature, the energy dissipation of the C_{60}@CNT system mainly occurred at both end edges of the CNT, where the C_{60} molecule is under restoring (or sucking-in) forces and the velocity direction of the C_{60} molecule is changed. However, the energy dissipation of the C_{60}@BNNT was caused by the collisions against the BNNT wall as well as at both end edges of the BNNT.

References

[1] Smith B W, Monthioux M and Luzzi D E 1998 *Nature* **396** 323
[2] Monthioux M 2002 *Carbon* **40** 1809
[3] Burteaux B, Claye A, Smith B W, Monthioux M, Luzzi D E and Fischer J E 1999 *Chem. Phys. Lett.* **310** 21
[4] Smith B W, Monthioux M and Luzzi D E 1999 *Chem. Phys. Lett.* **315** 31
[5] Smith B W and Luzzi D E 2000 *Chem. Phys. Lett.* **321** 169
[6] Hirahara K, Suenaga K, Bandow S, Kato H, Okazaki T, Shinohara H and Iijima S 2000 *Phys. Rev. Lett.* **85** 5384
[7] Sloan J, Dunin-Borkowski R E, Hutchison J L, Coleman K S, Williams V C, Claridge J B, Yorka A P E, Xu C, Bailey S R, Brown G, Friedrichs S and Green M L H 2000 *Chem. Phys. Lett.* **316** 191
[8] Kwon Y K, Tománek D and Iijima S 1999 *Phys. Rev. Lett.* **82** 1470
[9] Service R F 2001 *Science* **292** 45
[10] Berber S, Kwon Y K and Tománek D 2002 *Phys. Rev. Lett.* **88** 185502
[11] Qian D, Liu W K and Ruoff R S 2001 *J. Phys. Chem.* B **105** 10753
[12] Ulbricht H and Hertel T 2003 *J. Phys. Chem.* B **107** 14185

[13] Mickelson W, Aloni S, Han W Q, Cumings J and Zettl A 2003 *Science* **300** 467
[14] Okada S, Saito S and Oshiyama A 2001 *Phys. Rev.* B **64** 201303(R)
[15] Girifalco L A and Hodak M 2002 *Phys. Rev.* B **65** 125404
[16] Tersoff J 1988 *Phys. Rev.* B **38** 9902
[17] Tersoff J 1989 *Phys. Rev.* B **39** 5566
[18] Brenner D W 1990 *Phys. Rev.* B **42** 9458
[19] Ulbricht H, Moos G and Hertel T 2003 *Phys. Rev. Lett.* **90** 095501
[20] Albe K and Moller W 1998 *Comput. Mater. Sci.* **10** 111
[21] Kang J W and Hwang H J 2004 *Mater. Sci. Forum* **449–452** 1185
[22] Mayom S L, Olafson B D and Goddard W A III 1990 *J. Phys. Chem.* **94** 8897
[23] Kang J W and Hwang H J 2002 *Nanotechnology* **13** 503
[24] Kang J W, Seo J J and Hwang H J 2002 *J. Phys.: Condens. Matter* **14** 8997
[25] Kang J W and Hwang H J 2002 *J. Phys.: Condens. Matter* **14** 2629
[26] Allen M P and Tildesley D J 1987 *Computer Simulation of Liquids* (Oxford: Clarendon)
[27] Girifalco L A, Hodak M and Lee R L 2000 *Phys. Rev.* B **62** 13104
[28] Zhao Y, Ma C-C, Chen G H and Jiang Q 2003 *Phys. Rev. Lett.* **91** 175504
[29] Zheng Q, Liu J S and Jiang Q 2002 *Phys. Rev.* B **65** 245409
[30] Zheng Q and Jiang Q 2002 *Phys. Rev. Lett.* **88** 045503